Some Consideration on Shielding Effectiveness Testing by Means of the Nested Reverberation Chambers

Wojciech J. KRZYSZTOFIK[1], Robert BOROWIEC[1], Bartosz BIEDA[2]

[1]Dept. of Electronics Engineering, Wroclaw University of Technology, Wyspianskiego 27, 50-370 Wroclaw, Poland
[2] Nokia Siemens Networks, Strzegomska 56, 53-611 Wroclaw, Poland

wojciech.krzysztofik@pwr.wroc.pl, robert.borowiec@pwr.wroc.pl, bartosz.bieda@pwr.wroc.pl

Abstract. *This paper evaluates the effects of test fixture isolation when using nested mode-stir chambers for conducting electromagnetic shielding measurements. The nested chamber technique is used by both government and industry to evaluate the electromagnetic attenuating properties of materials as varied as infrared sensor windows to the composites used in the hulls of new ships, EM-protection of human as well as devices. Numerical simulation by means of CST and FEKO software of different nested chambers arrangements were done. Some preliminary test measurements of designed and manufactured small reverberation chamber were done and compared with the numerical simulation results.*

Keywords

Shielding effectiveness, planar screening material, measuring methods, nested reverberation chamber, numerical electromagnetic computational methods.
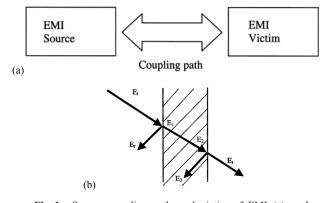
1. Introduction

Nowadays designers must consider various interference sources, such as licensed broadcasting transmitters, government equipment such as radars, nearby sources as wireless WLAN, Bluetooth, GSM/UMTS equipment, etc, the spectrum to be covered, typically 1 kHz-40 GHz, and threats prior to specifying a certain shielding requirement for a given installation. Threats may include lighting, electromagnetic pulse (EMP), and sensitive eavesdropping receivers. The use of radio frequency shielded enclosures has become quite common in our increasingly electromagnetically crowed environment. In many electromagnetic interference (EMI) problems, the important electronic systems are located within a metal enclosure with apertures. In such cases it is important to know the shielding effectiveness (SE) of the enclosure so that we can relate the interior fields to the external incident fields.

In every EMC problem we may distinguish three parts as shown in Fig. 1. These are the source of EMI, the victim of EMI and a coupling path. If at least one of these three parts is missing then we do not have an EMC problem.

Radiated interference is any interference transferred through space by an electromagnetic field. The level of interference is a function of directivity of the energy as it leaves the source, the losses on propagating to the device, the degree of coupling into, and the susceptibility of the device to the characteristics of the energy. In addition it depends on turbances, cosmic noise, solar radiation, and manmade sources such as automobiles, industrial, scientific, and medical equipment. Intentional Transmitters from LF communications to mobile, ground as well as satellite communication systems, and radars also can interfere with other services. Finally, two man-created threads of electronic eavesdropping and EMP must be considered.

Fig. 1. Source, coupling path, and victim of EMI (a), and wave approach to penetration through walls (b).

In many systems the outer skin (e.g., aircraft) or enclosure (e.g., equipment cabinet) forms part of an EM shield which contributes to the reduction of emission and susceptibility problems. A perfectly conducting shield without apertures or penetrations would be an ideal shield for all but low-frequency magnetic fields. However such an ideal is difficult to approach in practice. Invariably, shields are not perfectly conducting and have several openings and through wire connections. We focus on penetration through the walls of a shield due to its finite electrical conductivity. Another approach to diffusive shielding is based on the wave approach.

This approach is depicted in Fig. 1b where an incident electric field E_i is partially reflected from the wall E_r, partially penetrates E_1, reaches the other side of the wall after some attenuation E_2, suffers a partial internal reflection E_3, and part of it is transmitted into the inner region E_t. Component E_3 suffers further reflections (not shown) which contribute further to the transmitted wave. In complex problems, numerical solutions are necessary which employ special thin-wall formulations which also allow for inhomogenities and anisotropies.

It should be emphasized that although we have discussed shielding here by illustrating penetration from an outer region to an inner region, the reverse process follows the same rules (equivalence principle). In this and other shielding problems it is important to use the concept of shielding effectiveness (SE).

SE is defined as the ratio in dB of the field without and with the shield:

$$SE = 20\log\left|\frac{E_0}{E_t}\right|. \tag{1}$$

The SE of canonical shapes such as spheres, cylinders made out of various materials may be calculated analytically.

Knowing the power levels and location of interfering sources, a shielding effectiveness profile can be determined versus frequency and type of field for given protected barrier or complete enclosure. In a like manner, knowing the source of emissions from a data processing system, and the possible location and sensitivity of listening receiver, the amount of shielding effectiveness required for a given enclosure can be determined. In order to have some understanding of what is involved consider the following.

2. The SE Measurement Methods

The measurement of the shielding effectiveness (SE) of a planar material sample is required to predict the suitability of the material to form an enclosed electromagnetic shield. A typical shielded enclosure has an ultimate shielding performance that is limited by the shielding performance of its structural features such as apertures, penetrations and joints. For a high-quality shielded enclosure, the SE expressed logarithmically may exceed 100 dB when the enclosure is first commissioned.

Typical equipment enclosures, or enclosures that have a secondary shielding requirement, such as vehicle bodies, may have SE values in the range 10–80 dB. This lower performance is a consequence of the structural features, and the consequent requirement for the shielding performance of the structural material is lower, typically no more than 90 dB. Any sheet metal used as a structural material will have a SE considerably in excess of 90 dB. Structural materials formed from metalized plastic or other nonconducting substrates with an internal conducting component, such as reinforced carbon fiber composite (CFC), may

have SE values in the range below 90 dB and thus require measurement.

Such materials are conventionally measured in test systems that require a planar sample of the material to be placed across an aperture or within the cross section of a transmission line. Examples are the use of nested reverberation chambers (NRC) [1], [2], nested anechoic chambers, Faraday's cage, and coaxial transverse electromagnetic (TEM) waveguides cavity (Fig. 2), typically the standard ASTM cell [3].
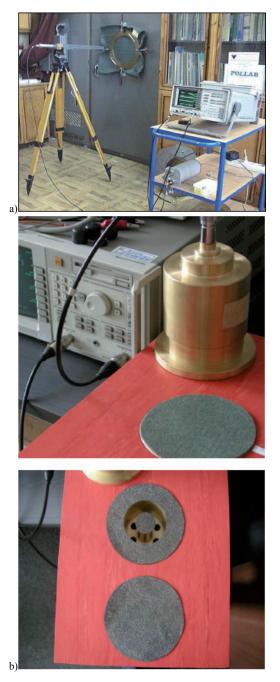

Fig. 2. The two examples of measuring setups of SE of membrane screening materials: the Faraday's cage (a), and coaxial transverse electromagnetic (TEM) waveguides cavity, at the EMC Laboratory of Wroclaw University of Technology (Poland).

In each of these systems, the measured reduction of transmitted electromagnetic energy (insertion loss) through the aperture or cell with the sample present is compared to that without the sample present and the data are processed to estimate the SE of the sample material. With the sample present, the energy flow is through the sample and possibly around the edge of the sample if a good conducting contact between the outer edge of the sample and the inner edge of the aperture/cell is not maintained along the entire sample perimeter. The edge contact requirement has been overcome in some coaxial systems [4], [5] but can be a major source of measurement error in other systems that require contact with a buried conducting material or samples with conductor on one side only. These problems are particularly acute as the frequency of the measurement increases and especially in the microwave frequency range where the structural dimensions of the sample material features, e.g., the weave in the fabric of a composite material, become comparable to the wavelength.

Over recent years, mode-stirred reverberation chambers have gained some popularity for measuring the shielding properties of materials. Originally developed at the Naval Surface Warfare Center (NSWC) in Dahlgren, Virginia, the technique is based on two nested chambers [6]. The material under investigation is placed over a window in the smaller chamber and thus, the amount of isolation between the two chambers can be measured. This paper shows that results obtained when the two chambers are tightly coupled may need further correction and offers both theoretical and experimental methods for doing so. Readers not acquainted with reverberation chambers are encouraged to read [6] and [7].

The purpose of this paper is to design the nested reverberation chambers setup, and model the shielding effectiveness of electrically large enclosures that contain apertures and interior loading.
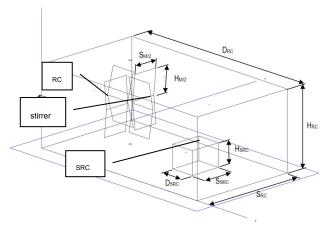
3. Preliminary Discussion

Before the nested chamber technique can be evaluated, the concept of shielding effectiveness must be quantified. In general, the shielding effectiveness of a material or configuration of materials (such as a screen imbedded in glass) is a measure of its ability to attenuate electromagnetic energy. This ability will depend upon both its reflection and absorption properties. Energy not being reflected or absorbed by the material will be transmitted from one side to the other. For a given material, the amount of energy transmitted has a complex dependence upon the angle of incidence and polarization of the incoming electromagnetic wave. It is assumed that the interest is in how the material will attenuate an isotropically impinging wave front (hence, the use of a mode-stirred chamber). Fig. 1b depicts a material being used to attenuate an isotropically impinging wave front originating from the left. A shielding factor, SE, will be defined as the total power per unit area,

S_{inc}, incident on the left side divided by the total power per unit area, P/A_w, leaving the right side.

4. Nested Chambers Theory and Design

4.1 Nested Chambers General Description

A typical nested chamber setup is shown in Fig. 3 [1]. A small reverberation chamber is placed inside a larger one. Both chambers use paddle wheels to stir the modes within each cavity. The smaller chamber has a window fixture used to mount the material of interest over an aperture and a receive antenna to measure the fields within, while the larger chamber uses a transmittal antenna to generate the reference fields. The shielding properties of the material of interest are measured by first leaving the aperture uncovered and measuring the power received inside the smaller chamber. The window is then covered with the material of interest and the received power is again measured. The ratio of these two numbers is then reported as the material's shielding effectiveness.

Parameter	Length D, m	Width S, m	Height H, m	Area A, m²	Volume V, m³
Reverberation Chamber, *RC*	7,76	4,34	3,09	142,135	104,07
Small Reverberation Chamber, *SRC*	0,98	1,24	0,90	6,43	1,09
Stirrer	-	4x1,00	2x1,05	8,4	-
Total	-	-	-	157	105,16

Fig. 3. Nested chambers configuration and their dimensions [8].

A closed cavity has many propagating modes which form 3-dimensional standing wave patterns with a large number of resonant modes (Fig. 4).

The modal resonance frequencies of a rectangular cavity are given by:

$$f_{m,n,l} = \frac{c}{2}\sqrt{(\frac{l}{D})^2 + (\frac{m}{S})^2 + (\frac{n}{H})^2}, \quad [Hz] \qquad (2)$$

where D, S, and H are the dimensions of the enclosure (in meters) (Fig. 3); m, n and l are integers, only one of which may be zero, and c is the propagation velocity of waves in the cavity, $c = 3.10^8$ m/s as in free-space.
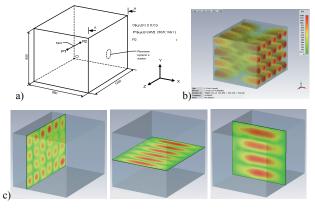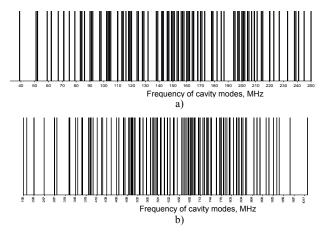

a)   b)

c)

Fig. 4. SRC geometry and excitation (a), 3-D E-field distribution (b), and in y-z, z-x, y-x planes (c) of TE$_{227}$ – mode (f_{LUF} = 0.998 GHz).

This gives raise to regions where the field is small and others where it is large. Typical variations are of the order of 40 dB, making the perceived test field very strongly dependent on the exact locations inside the cavity. At sufficiently high frequencies, the coupling between equipment and an antenna varies rapidly with position and frequency. When a large number of modes are present the field pattern becomes highly detailed (although regular), but there are still large and rapid variations in field with position and frequency (Fig. 5). The mode stirrers are used to alter the boundary conditions, thus moving the position of the maxima and minima of the field magnitude inside a chamber.

a)

b)

Fig. 5. Modal spectrum inside the empty RC (a), and SRC (b) as in Fig. 3.

The frequency above which the chamber operates according to the fundamental properties is assumed to be the lowest usable frequency, LUF. The LUF is generally determined by the effectiveness of the stirrer and the quality factor of the chamber. Its scope is about 3–5 times the first chamber resonance. In the IEC 61000-4-21 standard [1], it

is assumed to be the lowest frequency above which the field uniformity requirements are achieved. With another approach, the LUF is considered to be the frequency at which the chamber, due to the variable environment that is created by the movement of the stirrers, hosts an electromagnetic environment with 60 modes. For a rectangular enclosure the LUF can be determined by the following equation [7], [8]:

$$N = \frac{8\pi}{3}(\frac{f}{c})^3 DSH - \frac{f}{c}(D+S+H) + 0.5 \qquad (3)$$

where N is number of modes, f is the frequency of propagation, c is the wave speed of propagation, and D, S, H are the dimensions of the rectangular enclosure.

The modal density inside the chambers is described by:

$$\frac{\partial N}{\partial f} \approx 8\pi\, DSH\, \frac{f^2}{c^3} - (D+S+H)\frac{1}{c}\cdot \qquad (4)$$

The N and modal density $\partial N/\partial f$, for nested reverberation chambers, versus frequency dependence are shown in Fig. 6.
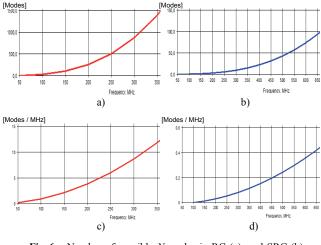

a)   b)

c)   d)

Fig. 6. Number of possible N modes in RC (a), and SRC (b) as well as the modes density $\partial N / \partial f$ in a RC (c) and SRC (d).

Equation (2), however, is a theoretical approach for determination of LUF, and an experimental verification should be performed each time a chamber calibration is done. As derived by (2), the LUF depends primarily on the chamber's dimensions as they define the modal structure as a function of frequency. A commonly accepted guideline sets the LUF border at the frequency where the minimum stirrer dimension is $\lambda/2$. However, the use of larger stirrer, apart from improving the field uniformity, may result in lower LUF. The dependence of the LUF on the chamber's dimensions, quality factor, and stirrer effectiveness can be conversely used, as for a given value of the LUF the minimum chamber requirements with regard to the later characteristics, can be specified. The working volume inside the chamber is thought to be placed at a distance of $\lambda/4$, at the LUF from any antenna, tuner, or other reflecting object.

4.2 Penetration through Aperture

A major route for penetration of EM radiation is through apertures. By this we mean any hole, opening, ventilation grid, imperfect joint which breaches the continuity of the conducting shield. It is normally the case that apertures form the major route for radiation breaching a shield. In general, the transmission cross section of an aperture depends on the incidence angle and polarization of the incident plane wave. Aperture penetration may be tackled in different ways depending on circumstances. These are based on small hole theory, simple analytical formulations for slots, intermediate level tools, and full numerical models.

We examine each approach below.

1. For holes that are electrically small we first calculate the electric field E_{sc} at the position of the whole assuming that the aperture has been replaced by a perfect conductor (short-circuit electric field). The presence of the aperture is then represented by placing an equivalent dipole inside the wall, where the aperture is again replaced by a perfect conductor. The dipole moment of the dipole is

$$p_e = 2\varepsilon\alpha_e E_{sc} \qquad (5)$$

where α_e is the hole electric polarizability.

As an example, the polarizability of a round hole of diameter d is $\alpha_e = d^3/12$.

The inner field can then be obtained by using antenna theory or any other suitable technique.

2. Alternative formulations have appeared in the literature where calculations of shielding effectiveness have been made for simple commonly encountered apertures. Particularly well known is the SE of a slot of length l:

$$SE = 20\log\frac{\lambda}{2l}. \qquad (6)$$

If the length of the slot is 1/10 of the wavelength then $SE = 14$ dB. Such performance at 1 GHz implies slot lengths smaller than 3 cm. Clearly, the shorter the length, the higher the SE. For the same area of aperture it is better to have several smaller apertures rather than one large one. The formula above for K apertures modifies to:

$$SE = 20\log\frac{\lambda}{2l\sqrt{K}}. \qquad (7)$$

Equations (6) and (7) do not take into account either the width of the slot or the presence of a resonant equipment enclosure hence they may result in large errors in SE estimates.

3. The cabinet and its apertures may be described using one of the full-field solvers described in [8]. For the case of a small number of electrically large apertures this process is straightforward. However, in the case of complex and extensive ventilation grids the computational effort required in describing and meshing a large three-dimensional problem is excessive. In such cases, techniques have been developed to calculate SE using full-field models with embedded digital signal algorithms describing the grid of apertures. Full-field calculation of SE in densely loaded cabinets, with several apertures, is still a very demanding computational task.

4.3 Effect of Chamber Isolation

The measured shielding effectiveness of a given window is defined by [1] as the ratio of the power density in the small chamber without the window installed to the power density in the small chamber with the window installed. It will first be assumed that the two chambers are tightly coupled with the window aperture uncovered. This condition will exist when the aperture is relatively large compared to the small chamber which, in practice, is assumed to have a high quality factor without the aperture. Thus, the power density in the small chamber with the window open, S_z, is approximately equivalent to the power density in the large chamber, S_l. Later, we will allow for the loosely coupled case where the window aperture provides some inherent isolation between the two chambers. It is also assumed that the difference in the loading of the large chamber by the small chamber, with and without the window installed, can be neglected.

Before we cut the aperture in the side wall of SRC we investigated the optimal position for it all over the wall. In Fig. 7 the surface current distribution for LUF i.e., the TE$_{227}$-mode, is shown.
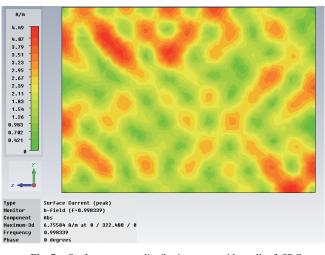

Fig. 7. Surface current distribution on a side-wall of SRC, f_{LUF}=0.998 GHz.

On the basis of surface current distribution we examined an optimal aperture position, and modeled the few of their shapes and dimensions situated as in Fig. 8.

An example of simulated current and power density inside the SRC, along the axis with aperture is shown in Fig. 9. In Fig. 10 the E-field distribution inside the nested reverberation chambers, for f_{LUF}=0,998 GHz is shown.
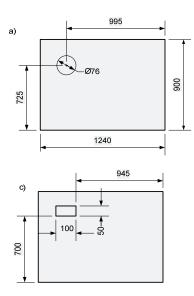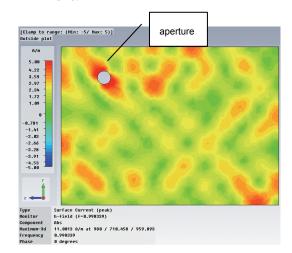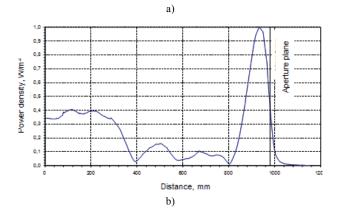
Fig. 8. Aperture shapes and dimensions in the side wall of SRC.

a)

b)

Fig.9. Simulated surface current (a), and power density (b) inside the SRC along the axis with aperture for aperture $\varnothing 76$, and $f_{LUF}=0.998$ GHz.
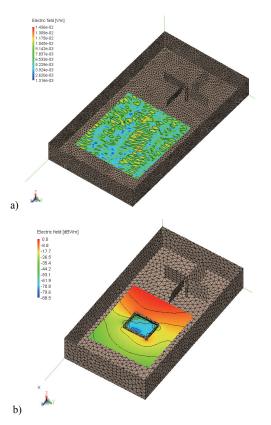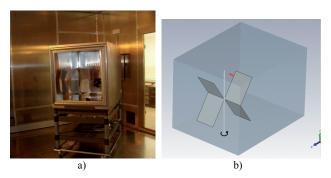

a)

b)

Fig. 10. E-field distribution inside the RC, and nested RC , $f_{LUF} = 0.998$ GHz.

4.4 Stirrer Influence on Field Distribution

As it is shown in Fig. 9, a field distribution is not even across the chamber, because it depends on an antenna placement, which excites the chamber. To have the biggest dynamic of the facility for shielding effectives the aperture should be cut out in the chamber wall in the area where the field is strongest. In such a case the aperture is the most exited and the maximum power leaks outside the chamber through the aperture and through the material under test when it covers the aperture. However, there is no way to guess where the strongest field is without extensive numerical computation. Prediction of the field distribution in the chamber is not needed if stirrer is applied inside. In Fig. 12-14 it is shown a current distribution on the side wall of the model of the chamber (Fig. 11). The chamber is exited by a monopole antenna mounted on the rear wall and disturbed with double wings stirrer.

Maximums of current and what is obvious the corresponding field moves across the chamber according to stirrer angular position. So, if stirrer is applied it doesn't matter where the aperture is placed on, because the maximum radiating power through the aperture can be found by adjusting the stirrer.

Fig. 11. Photo (a) and numerical model (b) of small reverberation chamber with double wings stirrer..
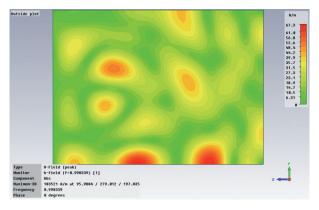

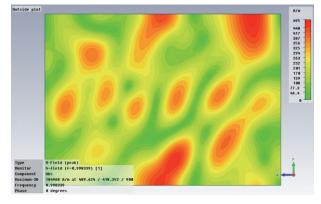**Fig. 12.** Current distribution on side wall. Stirrer at starting position.

Fig. 13. Current distribution on side wall. Stirrer rotated 45 degrees.
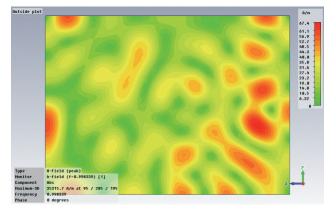

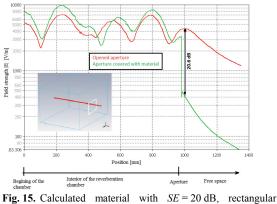**Fig. 14.** Current distribution on side wall. Stirrer rotated 90 degrees.

4.5 Calculation of Shielding Effectiveness of Material

The chamber model was used to calculate shielding effectives (SE) of a material with arbitrary chosen parameters: relative permittivity $\varepsilon_r = 4$ and conductivity $\sigma = 28.3$ S/m. Thickness of the sample was assumed on 2 mm. The material parameters were calculated form equations written in Balanis' book [9] to have SE=20 dB. Additionally SE of the material was confirmed by numerical calculations performed with coaxial line filled with the same sample of material.

The calculations by means of reverberation chamber were performed according to equation (1) with using CST software. First the electrical field was calculated for model chamber with opened aperture and then aperture was covered by 2mm sheet of material. Two square apertures with edge length 10 and 30 cm were taken under considerations. Calculated electric field strength along normal to the aperture is shown in Fig. 15 and Fig. 16.

The field decreases rapidly when crosses the attenuation material. Unfortunately the slump is slightly bigger than assumed attenuation of the material.

Computations were made only for one frequency and for rather small frequency because of numerical complexity due to large electrical dimensions of the chamber.

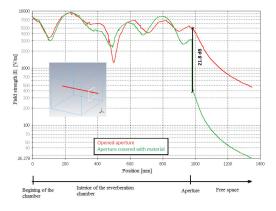**Fig. 15.** Calculated material with $SE = 20$ dB, rectangular aperture size 30×30 cm, $f = 998.3$ MHz.

Fig. 16. Calculated material with $SE = 20$ dB, rectangular aperture size 10×10 cm, $f = 998.3$ MHz.

5.   Preliminary Measurements of SRC

The chamber which is under consideration was manufactured (Fig. 17) and now is being under tests to discover its behaviors. Till now several measurements were done to improve the shielding effectives of the chamber. A few mechanical problems had to be solved to seal the chamber and achieve shielding effectives over 130 dB. The tightness of the chamber is very important. When the shielding effectiveness is week there is no possibility to measure materials with high attenuation because the leakage of the chamber is measured instead of the material under test.

To evaluate the future site dynamic and the chamber transmission ability, a simple test was performed. The internal corner of the chamber opposite to aperture was illuminated with horn antenna HF906. The energy transfer through the aperture was measured by means of antenna HF906 located 3 meters away from the aperture outside the chamber. Gain of both antennas is 7 dBi at 1 GHz.
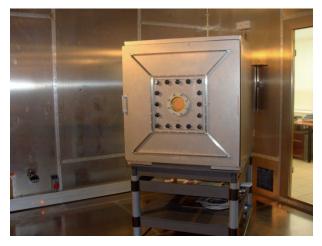

Fig. 17. Small reverberation chamber with a circular aperture at side wall.

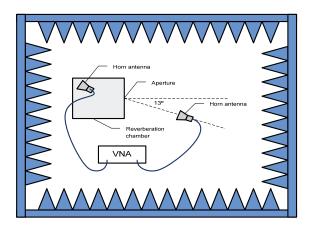A drawing of the test bed is shown in Fig. 18.

Fig. 18. Test bed for transmission measurements.

Measurements were done in a 10m anechoic chamber with a ground floor for different apertures in wide frequency band, but only two results for aperture with size

10x10 cm were presented as an example (Fig. 19, Fig 20). The transmission measurements were performed with Agilent 5701C vector network analyzer with 70 kHz bandwidth filter selected.

To discover dependencies between resonances of the chamber and energy being radiated outside reverberation chamber through the aperture the curves S_{21} were visualized in the same figures with resonance frequencies of the chamber. Moreover the curve for free space attenuation for three meters distance was added.

Based on information visualized on charts it can be noticed that not all modes propagate outside the chamber. There are frequencies equal to chamber modes at which signal vanishes outside the chamber and deep null appears.
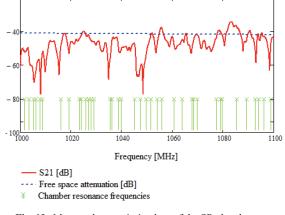

Fig. 19. Measured transmission loss of the SR chamber.

6.   Conclusions

In this paper, we have presented a nested reverberation chamber technique for measuring the shielding effectiveness of materials. This approach accounts for effects of both aperture and cavity size. The objective of the reverberation chamber is to obtain a field which is constant on average, which has many polarizations directions, and which is statistically uniform. In [3] a reverberation chamber test procedure has been given using a nested chamber, as shown in Fig. 2. This method needs a much higher frequency for proper operation due to the limited size of the test fixture, compared to the other method. A 3-D simulation (based of an EFIE-MoM approach in FEKO as well as in CST Studio solvers), of an RC and the nested RC's was used and presented in this paper. Calculation results allow to state, that closer results to real material attenuation are for electrically bigger apertures.

Acknowledgements

framework of the Operational Programme Innovative Economy. Authors wish to thank Mr Jaroslaw Janukiewicz from WRUT for delivering results of SRC measurements.

References

[1] International Electrotechnical Commission, *Testing and Measurement Technique-Reverberation Chamber Test Methods, Standard* 6100-4-21, 2003.

[2] HOLLOWAY, C.L., HILL, D.A., LADBURY, J., G., KOEPKE, R. GARZIA, Shielding effectiveness measurements of materials using nested reverberation chambers. *IEEE Trans. Electromagn. Compat.*, May 2003, vol. 45, no. 2, p. 350-356.

[3] American Society for Testing and Materials, *Standard Test Method for Measuring the Electromagnetics Sheilding Effectiveness of Planar Materials*. Standard D4935-99, 1999.

[4] CATRYSSE, J., DELESIE, M., STEENBAKKERS, W. The influence of the test fixture on shielding effectiveness measurements. *IEEE Trans. Electromagn. Compat.*, Aug. 1992, vol. 34, no. 3, p. 348-351.

[5] SARTO, M.S., TAMBURRANO, A. Innovative test method for shielding effectiveness measurement of conductive thin film in a wide frequency range. *IEEE Trans. Electromagn. Compat.*, May 2006, vol. 48, no. 2, p. 331-341.

[6] HATFIELD, M. O. Shielding effectiveness measurements using mode stirred chambers: A comparison of two approaches. *IEEE Trans. Electromagn. Compat.,* Aug. 1998, vol. 30, no. 3.

[7] CRAWFORD, M. L., KOEPKE, G. H. Design, evaluation, and use of a reverberation chamber for performing electromagnetic susceptibility/vulnerability measurements. *NBS Tech. Note 1092*, Apr. 1986.

[8] KRZYSZTOFIK, W. J., BOROWIEC, R., BIEDA, B. Optimization of nested reverberation chambers setup for shielding effectiveness measurements. *Scientific Report*, Nr I-28/09/S/107, *Wroclaw University of Technology, Wroclaw, Poland*, 2009.

[9] BALANIS, C. A. *Advanced Engineering Electromagnetics*, John Wiley & Sons, Inc., New York, 1989, p.235.

[10] KRZYSZTOFIK, W.J., BOROWIEC, R., BIEDA, B. Design consideration of nested reverberation chambers for shielding effectiveness testing. In *20th Int. Conf. on Applied Electromagnetics and Communications*. ICECom-2010, Dubrovnik(Croatia), 2010.

About Authors ...

Wojciech J. KRZYSZTOFIK received the M.Sc., and Ph.D. degrees from Wroclaw University of Technology, Wroclaw, Poland, both in electrical engineering, in 1974 and 1983, respectively. In 1974 he joined the Institute of Telecommunications, Teleinformatics & Acoustics, at the Faculty of Electronics Engineering of the Wroclaw University of Technology, WRUT, Poland, where he is currently an Associate Professor. Dr. W.J. Krzysztofik was a Vice Dean of the Faculty of Electronics Engineering at WRUT, Wroclaw from 2002 till 2005. His research interests include the microwave remote sensing, microwave applications in mobile communication, electromagnetic theory and computational electromagnetic methods applied to scatterers and antennas of arbitrary shape placed in complex environments. He has already published over 100 papers in various journals, conference proceedings, and is the author of the book "*Terminal Antennas of Mobile Communication Systems-Some Methods of Computational Analysis*", and co-author of the Artech House book "*Multiband Integrated Antennas for 4G Terminals*". He is a member of the WRUT scientific group engaged in the European projects: COST 297 "High Altitude Platforms for Communications and Other Services", and COST ASSIST (IC0603) „Antenna Systems & Sensors for Information Society Technologies", and in 2006 he joined the European Antenna Centre of Excellence. Dr. Krzysztofik is in the board of reviewers of several international journals including the IEEE Transaction on Antennas and Propagation, IET Microwave, Antennas and Propagation, as well as many conferences and symposia.

Robert BOROWIEC was born in Walbrzych, Poland, in 1968. He received the M.Sc. and Ph.D. degrees from the Wroclaw University of Technology, Wroclaw, Poland, in 1993 and 1998, respectively. Since 1998, he has been with the Radio Department, Institute of Telecommunications, Teleinformatics and Acoustics, Wroclaw University of Technology, where he is currently an Assistant Professor. His research interests focus on electromagnetics, microstrip antenna theory and technology, antenna arrays, measurement techniques.

Bartosz BIEDA was born in Świdnica, Poland, in 1984. He received the M.Sc. degree from the Wrocław University of Technology, Wrocław, Poland, in 2008. Since 2008, he has been with the Radio Department, Institute of Telecommunications and Acoustics, Wrocław University of Technology, where he is currently a Ph.D student. His research interests focus on numerical approach in electromagnetism.